

# Modification of radiation hardness of silicon *p-n* junction photodiodes by hydrogen plasma treatment

A. M. SAAD, A. V. MAZANIK  
*Belarusian State University, F. Skaryna av. 4, 220050 Minsk, Belarus*

A. K. FEDOTOV\*  
*Al-Balqa Applied University, P.O. Box 2041, 11953 Amman, Jordan*  
*E-mail: fedotov@bsu.by*

A. A. PATRYN  
*Technical University of Koszalin, Sniadeckich str. 2, 75-453 Koszalin, Poland*

S. V. CHIGIR, N. A. DROZDOV, A. I. STOGNIJ  
*Belarusian State University, F. Skaryna av. 4, 220050 Minsk, Belarus*

The influence of treatment by a low energy hydrogen ions on degradation of the spectral response, diffusion length of minority carriers ( $L_D$ ) and efficiency ( $\eta$ ) of silicon *p-n* junction photodiodes (solar cells without antireflective coatings) under the effect of electron irradiation has been investigated. Evaluation of the radiation hardness was made by subjecting the unhydrogenated and hydrogenated photodiodes to 1 MeV electron irradiation with doses of  $(0.1 \div 3) \times 10^{15} \text{ cm}^{-2}$ . The measurements have shown that pre-hydrogenation of the silicon *p-n* junction devices significantly decreases the degradation rate of  $L_D$  and  $\eta$  thereby improving their radiation hardness.

© 2005 Springer Science + Business Media, Inc.

## 1. Introduction

Development of highly-effective silicon solar cells (SCs) or photodiodes (PDs) with improved performance and responsivity is one of the important tasks of modern silicon material science and silicon-based devices engineering.

To improve the electrophysical characteristics of silicon material and efficiency of SCs/PDs, passivation of the structural defects is usually used [1, 2]. For crystalline silicon that can have a number of grown-in defects or defects induced by the technological process, the passivation by atomized hydrogen improved its electrical parameters [2, 3].

Silicon and silicon-based devices operating in space or under hard irradiation conditions will suffer a reduction/degradation in their parameters. Degradation caused by space radiation is the most significant factor in reducing SCs efficiency and SCs/PDs responsivity [4–8]. The damage caused by radiation particles in space is expressed as degradation of short circuit current (due to the decrease of minority carrier diffusion length) and responsivity. The main effects of radiation damage to SCs/PDs array are atomic displacements and ionization. Atomic displacements from normal lattice positions may form stable radiation damages which change the equilibrium carrier concentration and reduce minor-

ity carrier lifetime and diffusion length due to trapping and recombination phenomena [9–11]. Ionization may cause reduction of transmittance in SCs/PDs cover slides due to formation of colour centers in the glass or oxide material owing to the excitation of an orbital electrons which may be trapped by impurity atoms to form charged defect complexes and electron–hole pairs (e-h). The e-h pairs generated by the ionizing radiation cause additional photocurrents similar to solar illumination.

As has been shown in [3], the SCs/PDs irradiation hardness problem can also be solved (partially) by using hydrogen plasma treatment. The aim of this paper is to investigate the influence of treatment by low energy hydrogen ions and subsequent electron irradiation on the spectral response, diffusion length of minority carriers  $L_D$  and other properties of silicon *p-n* junction devices.

## 2. Experimental work

*p-n* junction devices (samples) were manufactured here using boron doped Czochralski (Cz) crucible grown single crystal substrates of resistivity of 0.5–3  $\Omega\text{cm}$ . The quality of the substrates was estimated by diffusion lengths of minority carriers  $L_D$  that were in the

\*Author to whom all correspondence should be addressed.

range of 25–400  $\mu\text{m}$ .  $p$ - $n$  junctions devices were manufactured using a standard screen-printed commercial solar cell design [12]. The wafers, have surface area of  $100 \times 100 \text{ mm}^2$  and 450  $\mu\text{m}$  thick, were subjected to cleaning, saw damage etching and texturization in caustic solution. Then  $p$ - $n$ -junction was formed at a depth of 0.45  $\mu\text{m}$  by thermal diffusion of phosphorous at the temperature of 900°C. Contact metallization was made on the devices by silver screen-printing technique. Every device was cut to 4 equal parts i.e.  $50 \times 50 \text{ mm}^2$  before hydrogenation and no antireflective (AR) coating was made on the surface of the samples. Note that the efficiencies of referenced  $p$ - $n$  junction solar cells manufactured by the same technology and covered with AR coatings were between 13.5 and 14%.

The hydrogenation was carried out in the setup used for ion-beam treatment, as shown in Fig. 1, with ion energy of 50–4000 eV [13] and a special wide-aperture ion source was developed for this purpose. The ion source contains an anode and a hollow cathode with one additional extracting grid (extractor) placed at the opposite end to the anode. Construction of the source was designed to locate the hydrogenated samples outside the plasma discharge region, to vary the energy of hydrogen ions over a wide range and to extract ions from plasma by the application of different bias voltages. Owing to the setup used four sets of samples were processed simultaneously and that made it possible to vary duration of the ion-beam treatment for different samples keeping the same conditions of vacuum and gas mixture.

Light current-voltage (I-V) characteristics before and after hydrogen plasma treatment and before and after irradiation were measured for the SCs/PDs devices under illumination conditions appropriate to the ?? 1.5 standard. The efficiency and other solar cell parameters were extracted from the light I-Vs by means of a standard procedure described in [14].

The diffusion length  $L_D$  of minority carriers was estimated from the spectral dependence of photoresponse (quantum efficiency) of  $p$ - $n$  junctions SCs/PDs in the spectral region from 900 to 1000 nm according to the expression derived in [15]

$$I_{\text{ph}} = \frac{K \Phi \lambda \alpha L_D}{(1 + \alpha L_D)},$$

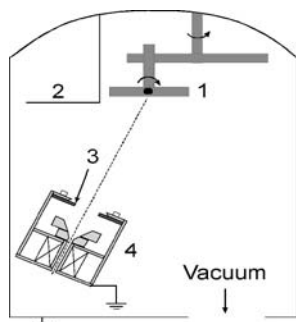


Figure 1 Hydrogenation setup: 1—substrate, 2—mobile diaphragm, 3—additional screen, 4—low-energy ion source.

where  $I_{\text{ph}}$  is the photocurrent,  $\Phi$ —light intensity,  $\lambda$ —wave length,  $\alpha$ —light absorption coefficient,  $K$  is a constant.

In order to predict the likely degradation of SCs/PDs in orbit it is a common practice to use the concept of an equivalent 1 MeV electron fluence/15 krad [16]. For this goal after the hydrogen plasma treatment the devices were irradiated with 1 MeV electron of fluences of  $1 \times 10^{14} \text{ cm}^{-2}$ . The same devices were then irradiated several times with the same particle and energy but for total dose of  $3 \times 10^{14}$ ,  $1 \times 10^{15}$  or  $3 \times 10^{15} \text{ cm}^{-2}$  to simulate different stages of space radiation.

### 3. Results and discussion

Different SCs/PDs samples have a slightly distinguished initial characteristics and therefore the normalized differences in  $L_D$  and  $\eta$  were used to characterize the influence of hydrogen plasma and electron irradiation. For hydrogenation experiments these normalized characteristics are equal to  $(L_D - L_{D0})/L_{D0}$  and  $(\eta - \eta_0)/\eta_0$ , where  $L_{D0}$  and  $\eta_0$  are initial values of diffusion length and efficiency respectively.

Fig. 2 shows the normalized difference in efficiency  $(\eta - \eta_0)/\eta_0$  of the devices versus ion energy  $E$  of the hydrogen plasma after the hydrogenation at temperature of 40–350°C for 5–15 min. The figure shows the strong dependence of the normalized difference in  $\eta$  on the energy of hydrogen ions, i.e. the normalized difference in  $\eta$  decreases as the ion energy increases. Fig. 2 shows that for substrates with the initial diffusion lengths between 100 and 250  $\mu\text{m}$  the ion energy of less than 200 eV is the most appropriate value to the improvement of  $\eta$ .

The observed dependence  $\eta(E)$  means that the hydrogenation is accompanied not only by the passivation of the structural defects but also by some other effects responsible for the variation of SC/PD performance.

To evaluate the nature of such behavior the influence of hydrogen plasma treatment (using the same regimes as for SC/PD devices) onto the surface structuring and minority carriers mean lifetime changes in the initial (non-textured) substrates was studied.

In these experiments Cz-Si substrates of 10  $\Omega\text{cm}$  and boron doped were treated by the atomized hydrogen beams with the energies of 50–800 eV at 30°C for

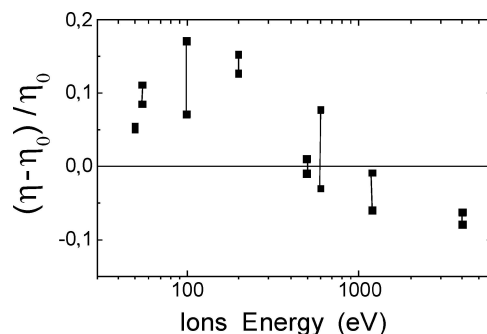


Figure 2 Normalized change in the efficiency versus ion energy, for the devices treated in hydrogen plasma at temperature of 40–350°C for 10–15 min.

exposure times of 5 to 40 min. Patterns of the structuring and surface roughness were studied using SEM and AFM devices. SEM measurements were done on a LEO 440 and AFM measurements were conducted on FEMTOSCAN-001. Character of the texturization of the treated surface was estimated by the comparison of the Root Mean Squared (RMS) roughness for the untreated and treated surfaces using samples of different regimes. The mean lifetime ( $\tau$ ) of carriers was estimated using the method of decay of photoconductance kinetics with excitation by 930 nm light.

Our measurements have shown that hydrogen plasma treatment of the samples always transforms the surface from atomically-smooth (with 0.2 nm RMS-roughness for initial wafers) into nano-structured pyramide-like patterns giving rise to RMS-roughness. Moreover, the highest structuring of wafer surface occurred at the first 5 min of hydrogen treatment so RMS-roughness reached 0.4, 1.2 and 1.4 nm corresponding to the hydrogen ion energies of 100, 400 and 800 eV respectively. The further increase of exposure time to 40 min resulted only in the surface evening-out and the decrease of RMS-roughness down to 0.2–0.3 nm regardless to the energy of the beam. The behavior of  $\tau(t)$  dependencies is also strongly dependent on the energy of hydrogen atoms. The value of  $\tau$  for the low energies of 50–100 eV had dropped sharply from its initial averaged value of 20 to 13  $\mu\text{s}$  for the first 5 min of treatment and then increased to  $\sim 19 \mu\text{s}$  after 40 min of the treatment. However, for high energies (200–800 eV) and after sharp drop for the first 5 min  $\tau$ -value continued to decrease as the treatment continued.

These additional experiments confirm that hydrogenation of the devices by the used regimes was accompanied not only by the passivation of the structural defects and also resulted in the structuring of the surface (that can decrease  $\tau$  and  $L_D$  in under-surface part of the wafers and increase  $\eta$ ) and introducing nearsurface defects (that can decrease  $\tau$  and  $L_D$  in under-surface part of the wafers). The surface relief modification by the ion beam can lead to additional light absorbtion in the  $p$ - $n$  junction device and hence to the efficiency enhancement under hydrogen plasma treatment despite the decrease of  $\tau$  and  $L_D$ . Note that structuring of the surface relief and introduction of the sub-surface defects due to hydrogen plasma treatment of silicon were also observed in [17].

Fig. 3 shows that the normalized change in efficiency of the devices is strongly dependent on the exposure time and temperature of the hydrogenation process. In particular, for the lowest temperatures (40 to 240°C) a maximum increase of  $\eta$  was observed only for 5–20 min exposure time. However, for the hydrogenation process of temperature of 340°C a maximum effect was not obtained even for 40 min exposure time, Fig. 3.

The above described behavior of the  $\eta(t)$  dependence indicated that an increase of exposure time is not constantly convenient condition for the improvement of SCs/PDs performance. The authors believe that accumulation of hydrogen for the devices treated at the low temperature resulted in suppression of  $L_D$  (and  $\eta$ ) due to the generation of hydrogen—related defects in the

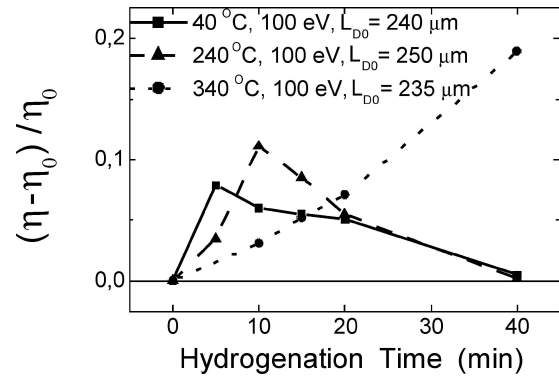


Figure 3 Normalized change in the efficiency versus hydrogenation exposure time for the devices which were treated in hydrogen plasma at temperatures of 40°C, 240°C and 340°C for 5–40 min.

layer beneath the  $p$ - $n$  junction. Shift of the  $\eta$  maximum with higher exposure time and with an increase of hydrogenation temperature is probably due to the enhancement of hydrogen diffusivity confirming the above-mentioned assumption.

To check experimentally the idea of the radiation hardness improvement due to hydrogenation of the devices, the initial (unhydrogenated) and hydrogenated samples were irradiated by 1 MeV electrons. The results of these experiments are presented as follows:

Table I shows  $L_D$  values as influenced by the hydrogenation process (ion energy of 100 eV, ion beam current density of 0.1 mA/cm<sup>2</sup>, 260°C) and the subsequent of 1 MeV electron irradiation with a dose of  $2.25 \times 10^{14} \text{ cm}^{-2}$ . For this experiment the  $p$ - $n$  junctions were manufactured on unhydrogenated substrates with average value of the (initial) diffusion length of  $\sim 100 \pm 10 \mu\text{m}$ . The hydrogenation at this temperature did not lead to the radiation hardness improvement i.e.  $L_D(t)$  for both of unhydrogenated and hydrogenated samples decreased under irradiation in the same manner. Similar results were obtained for the hydrogenated devices at room temperature which led to a further set of experiments to be carried out at higher temperatures.

Fig. 4 shows the normalized changes in diffusion length  $\{L_D(D) - L_D(0)\} / L_D(0)$ ,  $L_D(0) = L_D$  for a dose  $D = 0$  (i.e.  $H$  state), under hydrogenation at 340°C, 100 eV, 0.1 mA/cm<sup>2</sup> for different times and the subsequent electron irradiation. The changes in quantum efficiency upon electron irradiation of the samples are shown in Figs 5 and 6.

TABLE I

Time of Hydrogenation (min)	$L_D$ ( $\mu\text{m}$ ) of the devices correspond to their states		
	Initial	Hydrogenated	Irradiated by 1 MeV electrons
0	99	–	30
5	110	130	32
10	90	135	34
15	104	125	34
20	104	105	30
40	98	90	32

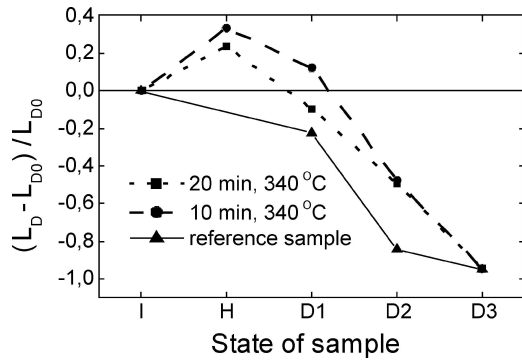


Figure 4 Normalized changes in diffusion lengths for the hydrogenated and the subsequent 1 MeV electron irradiated samples: States of the devices on the abscissa: I—initial (before hydrogenation), H—after hydrogenation, D1 → D3: after electron irradiation with total doses of (cm<sup>-2</sup>) i.e., D1 = 1 × 10<sup>14</sup>, D2 = 3 × 10<sup>14</sup>, D3 = 1 × 10<sup>15</sup>.

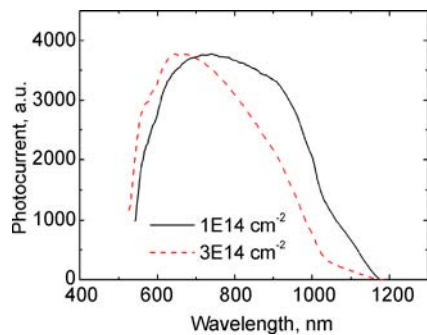


Figure 5 Quantum efficiency (normalized to its maximum) versus wavelength for the reference (unhydrogenated) devices irradiated with different doses of electrons.

Figs 4 to 6 show that hydrogenation led to the increase of  $L_D$  (points of H state in Fig. 4). Under electron irradiation the degradation of  $L_D$  took place for both of the hydrogenated and reference samples (points of D1 to D3 states in Fig. 4). Fig. 4 shows two peculiarities of the diffusion length behavior under irradiation and that attracted the attention as follows: Firstly, electron irradiation caused monotonous degradation of the diffusion length for doses up to  $3 \times 10^{14} \text{ cm}^{-2}$ . Figs 5 and 6 show that the quantum efficiency has decreased in the long-wave region of the spectrum. However, the  $L_D$  degradation rate over this range of doses is less for the hydrogenated samples than that for the reference devices by a factor of 3. Secondly, the diffusion length

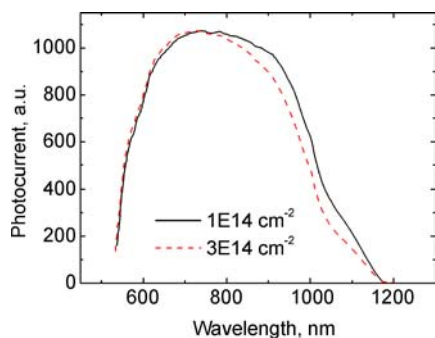


Figure 6 Quantum efficiency (normalized to its maximum) versus wavelength for the hydrogenated devices irradiated with different doses of electrons.

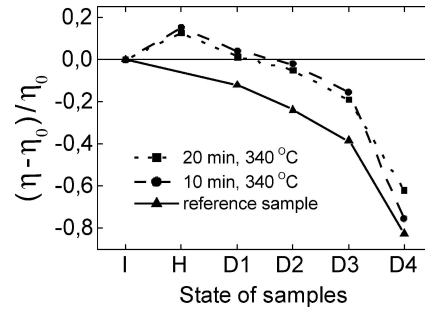


Figure 7 Normalized changes in the efficiency for the hydrogenated and the subsequent electron irradiated samples. States of the devices on the abscissa: I—initial (before hydrogenation), H—after hydrogenation, D1 → D4: after electron irradiation with doses of (cm<sup>-2</sup>) i.e. D1 = 1 × 10<sup>14</sup>, D2 = 3 × 10<sup>14</sup>, D3 = 1 × 10<sup>15</sup>, D4 = 3 × 10<sup>15</sup>.

for both of the hydrogenated and reference samples became approximately equal under irradiation with doses higher than  $1 \times 10^{15} \text{ cm}^{-2}$  (state D3 in Fig. 4).

Fig. 7 correlates qualitatively behaviors of the normalized changes in efficiency  $\{\eta(D) - \eta(0)\} / \eta(0)$ ,  $\eta(0) = \eta(D)$  for a dose  $D = 0$  (i.e. H state), with that of the normalized changes in diffusion length when the devices were subjected to hydrogenation followed by electron irradiation. In particular, for doses  $\leq 1 \times 10^{15} \text{ cm}^{-2}$  (state D3 in Fig. 7) the degradation rate of efficiency is less for the hydrogenated samples than that for unhydrogenated devices. At the same time, when the irradiation dose exceeded  $3 \times 10^{14} \text{ cm}^{-2}$ , the efficiency continued to degrade at very close rates for both of the hydrogenated and reference samples (state D4 in Fig. 7).

The presented results gave a direct evidence of the pre-treatment process, of silicon *p-n* junction samples, in low-energy hydrogen plasma which significantly improved the device radiation hardness. Moreover, in some cases such as for initially high- $L_D$  samples, this increase of radiation hardness were observed even when the hydrogenation resulted in the decrease of  $L_D$ .

The idea of improvement of silicon radiation hardness is based on the assumptions of work [18] and is as follows: During hydrogen plasma treatment of silicon wafers or silicon-based devices which are saturated by atomic hydrogen and that (atomic hydrogen) incorporated into silicon is partly transformed into the molecular state at temperature of 200–400°C, occupying the interstitial positions, and that does not influence the properties of the sample. The sample which operates under the irradiation conditions will have high densities of radiation defects (vacancies, interstitials, etc.) which can be introduced into its bulk. It had been shown in reference [18] that the generation of mobile vacancies in the vicinity of hydrogen molecules has resulted in their dissociation into two atomic constituents (owing to the field of elastic stresses near the defect). After the dissociation two unbonded hydrogen atoms become mobile and therefore can passivate the dangling bonds on radiation defects. This is just the enhancement of the radiation hardness. This effect of neutralization of radiation defect by plasma-introduced hydrogen was experimentally established in our earlier work [3] for monocrystalline silicon subjected to  $\gamma$ -irradiation.

#### 4. Summary

The obtained results have shown that the optimum selection of the hydrogenation parameters can enhance both of the diffusion length and efficiency of the single crystal silicon *p-n* junctions PDs/SCs i.e. the energy of hydrogen ions is a critical parameter for the efficiency. Temperature of the devices during hydrogen treatment had influenced the optimum exposure time of the hydrogenation. Hydrogenation process minimized significantly degradation rate of the diffusion length and quantum efficiency of the electron irradiated *p-n* junctions PDs/SCs for doses less than  $3 \times 10^{14} \text{ cm}^{-2}$ . Limitation of doses for the enhancement of radiation hardness due to pre-hydrogenation is likely due to depletion of the accumulated molecular hydrogen in the studied samples.

#### References

1. P. DE PAW, R. MERTENS and R. VAN OVERSTRAETEN, "Silicon Processing for Photovoltaics II," edited by C. P. Khattak and K. V. Ravi (N-HPP, 1987) Vol. 6, p. 1.
2. S. J. PEARTON, J. W. CORBETT and M. STAVOLA, "Hydrogen in Crystalline Semiconductors" (Springer-Verlag, Berlin, Heidelberg, New York, 1992).
3. A. FEDOTOV, A. MAZANIK and A. ULYASHIN, in Proceedings of the 10th Sede Boqer Symposium on Solar Electricity Production (Sede Boqer, Israel, February 4–5, 2001) 151.
4. L. DUSSEAU, T. L. RANDOLPH, R. D. SCHRIMPF and K. F. GALLOWAY, *J. Appl. Phys.* **81** (1997) 2437.
5. J. A. KEMMER, *Sensors and Actuators* **15** (1988) 169.
6. G. A. LANDIES and S. G. BAILEY, *ALP Conference Proceedings* **324(2)** (1995) 1011.
7. H. Y. TADA and J. R. CARTER JR., "Solar Cell Radiation Handbook" (JPL-Jet Propulsion Lab).
8. A. M. SAAD, *Canadian J. Phys.* **80** (2002) 203.
9. D. BIELLE-DASPET, J. BOURGOIN, J. BERNARD, L. CASTANER-MUNOZ, L. PRATT and R. L. CRABB, in Proc. 3rd Europ. Symp. Photovoltaic Generators in Space (ESA SP 173, Bath, 1982) p. 103.
10. T. MARKVART, T. J. GUMBERBATCH, M. W. WALKDEN and A. A. DOLLERY, in Proc. 3rd Europ. Symp. Photovoltaic Generators in Space (ESA SP 173, Bath, 1982) p. 109.
11. Z. RADZIMSKI, J. HONEYCUTT and G. A. ROZGONYI, *IEEE Trans. Electr. Dev., ED* **35(1)** (1988) 80.
12. J. F. NIJS, J. PORTMANS, S. SIVOTHAMAN and R. P. MERTENS, *ibid.* **46** (1999) 1948.
13. A. I. STOJNIJ and S. V. KORYAKIN, *Instr. Experim. Techn.* **43** (2000) 783.
14. A. L. FAHRENBRUGH and R. H. BUBE, "Fundamentals of Solar Cells. Photovoltaic Solar Energy Conversion" (Academic Press, New York, 1983).
15. D. L. LILE and N. M. DEVIS, *Solid State Electr.* **18** (1976) 699.
16. M. W. WALKDEN, in Proc. 3rd Europ. Symp. Photovoltaic Generators in Space (ESA SP 173, Bath, 1982) p. 95.
17. A. G. ULYASHIN, R. JOB, W. R. FAHRNER, O. RICHARD, H. BENDER, C. CLAEYS, E. SIMOEN and D. GRAMBOLE, *J. Phys.: Cond. Matt.* **14** (2002) 13037.
18. S. K. ESTREIHER, J. L. HASTINGS and P. A. FEDDERS, *Phys. Rev.* **57** (1998) R12663.